

See discussions, stats, and author profiles for this publication at: <https://www.researchgate.net/publication/231665090>

Ring Formation in Single-Wall Carbon Nanotubes

ARTICLE *in* THE JOURNAL OF PHYSICAL CHEMISTRY B · AUGUST 1999

Impact Factor: 3.3 · DOI: 10.1021/jp991513z

CITATIONS

110

READS

29

3 AUTHORS, INCLUDING:



Richard Martel

Université de Montréal

162 PUBLICATIONS **12,115** CITATIONS

SEE PROFILE



Phaeton Avouris

IBM, T. J. Watson Research Center

519 PUBLICATIONS **45,637** CITATIONS

SEE PROFILE

LETTERS

Ring Formation in Single-Wall Carbon Nanotubes

Richard Martel, Herbert R. Shea, and Phaedon Avouris*

IBM Research Division, T. J. Watson Research Center, Yorktown Heights, New York 10598

Received: May 6, 1999; In Final Form: July 14, 1999

Nanotube rings were fabricated from straight single-wall carbon nanotubes (SWNTs) with yields exceeding 50%. The rings result from the folding of nanotubes onto themselves under ultrasonic irradiation to form coils with a narrow distribution of radii (300–400 nm). A simple continuum elastic model is used to discuss the thermodynamic stability of the rings. Their formation involves a balance between tube-tube van der Waals adhesion and the strain energy resulting from the coiling-induced curvature. Our findings suggest that ring formation is a kinetically controlled process where bubble cavitation, generated by ultrasonic irradiation, provides the energy necessary to activate ring formation. The electrical conductance of the rings is measured as a function of temperature and in the presence of a perpendicular magnetic field. While the rings consist of bundles of many metallic and semiconducting SWNTs, they exhibit metallic behavior at low temperatures, and quantum interference effects are clearly observed.

Self-organization and the formation of molecular superstructures is a subject of strong current interest.^{1,2} This field is driven in part by a desire to understand the formation of biological structures such as proteins, cell membranes, etc., and in part by technological needs. As the push to increased miniaturization of structures and devices continues, conventional fabrication techniques are hard pressed to keep up, and self-assembly and self-organization techniques are sought to replace them.^{2,3} One of the most studied processes of self-organization is the coiling and ring formation by bio-polymers such as DNA and proteins.^{4,5} These processes are complex, involving a number of different types of interactions. Here we discuss a case of self-organization that involves coiling and ring formation by carbon nanotubes, materials known for their high flexural rigidity.^{6,7} Unlike the coils of bio-polymers that are usually stabilized through hydrogen bonding and ionic interactions, the coils of nanotubes are stabilized solely by van der Waals forces.⁸

Carbon nanotubes (NTs) are a new class of materials that

consist of one or several graphene sheets rolled up into a seamless tube, forming single-wall (SWNTs) or multiwall (MWNTs) nanotubes, respectively.^{9–11} NT's very high tensile strength is comparable to that of diamond,^{6,7} and depending on their atomic structure, NTs behave electrically as metals or as semiconductors.^{12–14} The synthesis of carbon nanotubes is itself a self-organization process, where carbon atoms self-assemble, with or without the help of catalysts, to form the tubes.^{15–17}

An important characteristic of carbon nanotubes is the strong van der Waals attraction between tubes, and between nanotubes and the substrate on which they are deposited. These van der Waals forces have important implications for the geometry and detailed configuration of the tubes. In the case of SWNTs, the van der Waals attraction between the NTs leads to a second level of self-organization; the nanotubes bunch together to form ropes, in which the NTs are closely packed in a triangular lattice.¹⁶ Within a rope, the tube-tube interactions are strong enough to induce radial deformation of the tubes.¹⁸ Similarly, van der Waals interactions with the substrate have been found to lead to both axial and radial deformations of adsorbed tubes and, most importantly, to stabilize highly strained nanotube

* Author to whom correspondence should be addressed. E-mail: avouris@us.ibm.com.

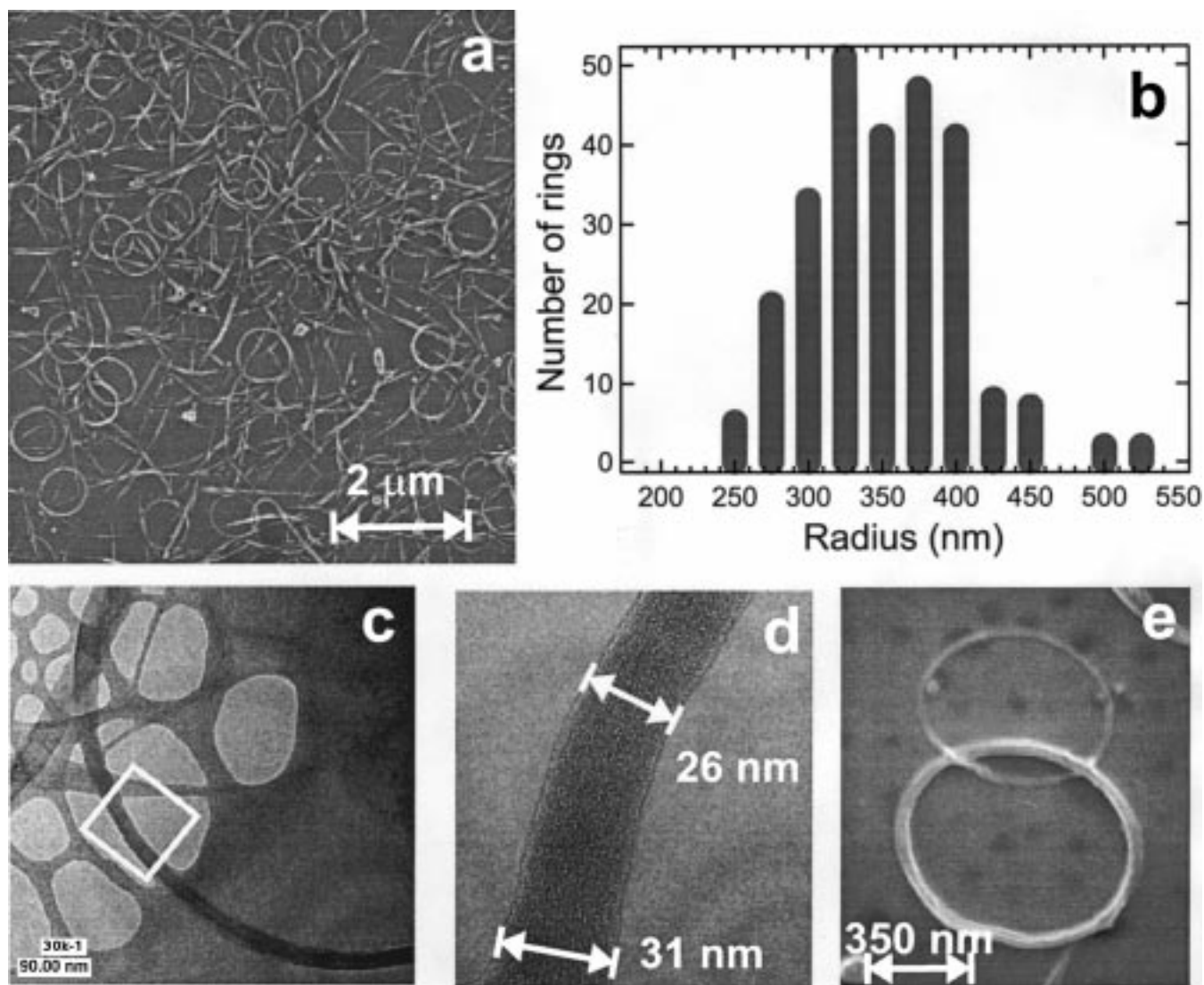


Figure 1. Characterization of rings of single-wall nanotubes (SWNTs). (a) Scanning electron microscope (SEM) images of a ring-containing SWNT sample dispersed on an hydrogen-passivated silicon substrate. The rings are produced by the process discussed in the text which transforms up to 50% of the raw material. (b) Histogram obtained from the analysis of many SEM images showing the distribution of the radii of the rings. (c) and (d) Transmission electron microscope (TEM) images of a SWNT ring dispersed on a holey carbon substrate (courtesy of Lynne Gignac). Variations of the diameter of the rope along its circumference (as seen in 1d) can be detected in most of the rings. The fringes result from the presence of individual nanotubes and the spacing is typical of a rope of SWNTs. (e) SEM images of two interlocked rings.

configurations.^{19,20} The latter allows the manipulation of their shape with the tip of an atomic force microscope (AFM).^{19,21}

We found conditions under which the same strong adhesion forces between SWNTs can generate yet another self-organized state that involves the formation of well-defined ring (coil) configurations. Starting with straight SWNTs and following the procedure described below, we succeeded in forming rings with yields as high as 50%. Their formation involves the ultrasound-driven self-folding of SWNTs, and their stability is due to the attractive van der Waals forces between the nanotubes. Simple arguments based on continuum elasticity theory bring insight into the factors that control the ring formation process.

Our preparation of SWNT rings involves the processing of raw material of SWNTs fabricated by laser vaporization.¹⁶ This technique produces long and entangled SWNTs with an average diameter of about 1.4 nm. To form the rings we start with 0.4 mg of such raw SWNTs in 8 mL of a mixture of concentrated sulfuric acid and hydrogen peroxide ($\text{H}_2\text{SO}_4/\text{H}_2\text{O}_2$ (10–30%)) in a 9:1 ratio) and irradiate them with ultrasound for 1–3 h (40 kHz, 190 W) at 40–50 °C. This oxidative treatment disperses the SWNTs, reduces the amount of residual metal catalysts and

amorphous carbon deposits, and decreases the length of the nanotubes ropes.²² After sonication, the nanotube solution is filtered through a 0.2 μm membrane filter. The residue is rinsed using DI water and dried in air. The NTs are then suspended in 1,2-dichloroethane using a brief period of sonication with low-power ultrasound [~ 100 W]. This process generates a stable suspension of a mixture of SWNT rings and ropes.²³

The scanning electron microscope (SEM) image in Figure 1a shows an example of nanotube rings deposited on a passivated silicon surface. This picture clearly illustrates the high yield of rings produced by our procedure. To obtain such a high yield requires shortening the raw nanotubes to a length of the order of 3–4 μm. As a result, the yield varies with the time of exposure to ultrasound and the concentration of the peroxide solution. The measured distribution of the ring radii is shown in Figure 1b; most rings have radii in the range of 300–400 nm. Transmission electron microscope (TEM) images such as the ones in Figure 1c,d confirm that the rings consist of aligned ropes of SWNT. The observed fringes correspond to individual tubes forming the rope. Figure 1e shows a close

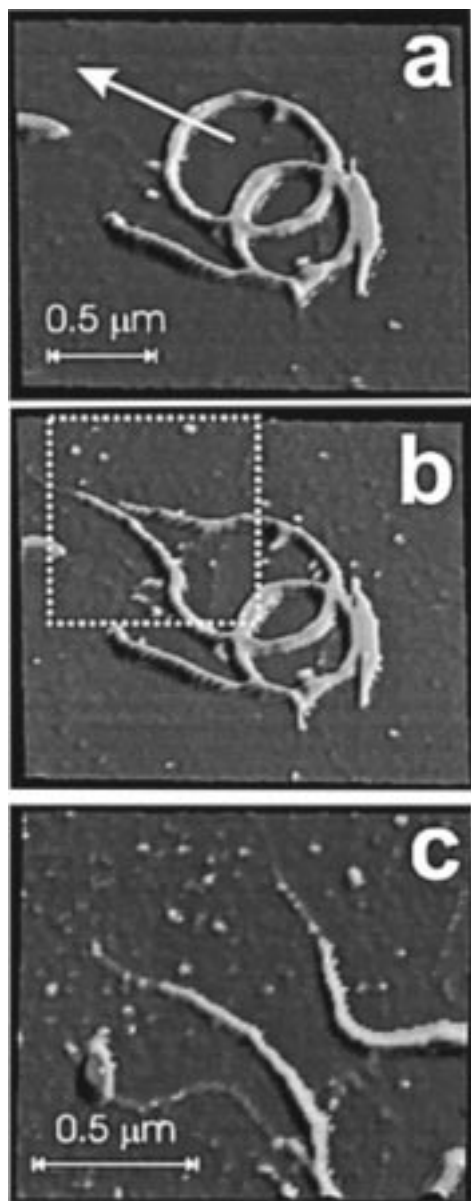


Figure 2. Noncontact AFM images of SWNT rings deposited upon a hydrogenated Si(100) surface. (a) Image of the rings before their manipulation with the AFM (b) and (c) sequence of manipulation to unfolded the ring structure into a single rope of SWNTs with two open ends. A vertical load of 30 nN was applied to the tip in order to unfold the ring.

up of two inter-locking rings, a catenane structure similar to those observed in DNA.²⁴

A priori, rings could be either coils or tori. A toroidal structure has covalent C–C bonds between C atoms at the two ends of a given tube, forming a hollow torus of carbon atoms. For such a torus, the ring circumference is exactly the initial tube length. In contrast, a coil structure, illustrated in the inset of Figure 3, corresponds to a tube forming a very tight spiral stabilized by the strong tube–tube van der Waals attraction. Tubes forming coils are significantly longer than the ring circumference.

The structure of rings, i.e., tori or coils, can be deduced on the basis of a number of observations. First, the fact that the starting material involves long SWNTs that are shortened by oxidation, which leaves the tube ends functionalized with carboxylic acid (COOH) groups,^{22,25} argues strongly against the formation of a torus involving covalent C–C bond linking. TEM

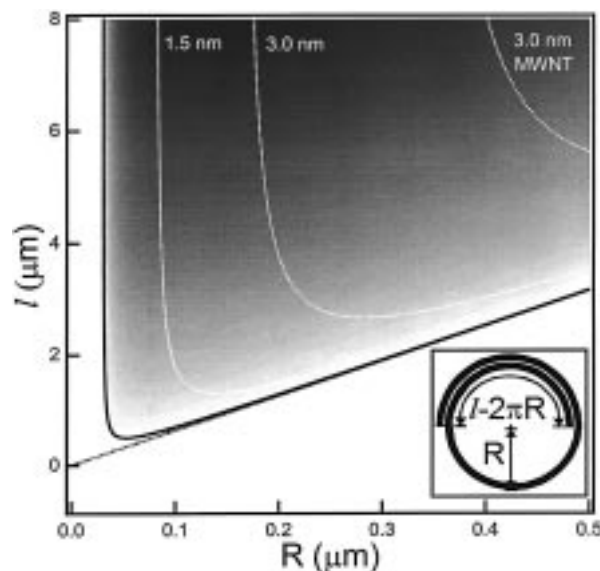


Figure 3. Thermodynamic stability limits for rings formed by coiling single-wall nanotubes with radii 0.7 nm calculated using the continuum elastic model described in the text where the cohesive energy per unit length K is 0.476 eV/nm¹⁸ and the wall thickness t is 0.2 nm. The total energy (sum of the strain and cohesive energies) is given in the gray image plot where the energy is scaled from dark gray to white with value ranging from −1870 to 0 eV, respectively. The overall gray area shows the range of ring radii allowed for a given length l of a single SWNT. Thermodynamic stability limits for nanotube rings with diameters of 1.5 nm ($t = 2.0$ nm), 3.0 nm ($t = 2$ nm), and 3.0 nm ($t = 3.0$ nm, i.e., a solid tube such as a MWNT) are also presented by the white dotted lines. These limits are calculated for $K = 0.839$ and 1.799 eV/nm for the 1.5 and 3.0 nm tubes, respectively.¹⁸ The inset is a schematic of a ring identifying the relevant parameters.

(see Figure 1c,d) and primarily AFM images indicate that the rings do not have a constant thickness and height around their circumference. This suggests that separate ropes curl together to form the rings. Further evidence for this comes from AFM tip manipulation experiments such as the example presented in Figure 2, where we find that it is relatively easy to take apart the rings and expose rope ends. Previous work,¹⁹ however, has shown that cutting single tubes or ropes with an AFM tip is nearly impossible: the tubes are simply translated. We thus conclude that the rings are indeed produced by a coiling process.

Images of the same batch of rings dispersed several months apart on Si wafers show similar concentration. In addition, short periods of sonication at low power of the ring solution do not seem to affect the ring stability. It is therefore clear that the rings are very stable in 1,2-dichloroethane.

Previously, trace quantities of rings have been observed by Liu et al.²⁶ while examining raw SWNTs made by laser ablation. They estimated the concentration of these rings to be 0.01–0.1% and assumed them to be perfect tori,²⁶ i.e., stabilized by covalent C–C bonds instead of van der Waals interactions. Our results suggest that they are more likely to be coiled NTs. There has been a report of SWNT rings formed during the evaporation of the solvent.²⁷ A small number of MWNT rings have also been identified in the raw material.²⁸ These MWNT rings were tentatively interpreted as segments of compressed helical nanotubes, i.e., consisting of sequences of straight segments of a nanotube followed by pentagon–heptagon pair defects that cause a bend in the nanotube. However, a toroidal structure could not be ruled out.²⁸ As is discussed below, MWNT rings with micron-sized diameters cannot be stabilized by van der

Waals forces only. Our results thus support the proposal that twisting pair defects must be present in the reported case of MWNTs.²⁸

Insight into the coiling process and the resulting size distribution of the rings is provided by simple considerations based on continuum mechanics. For the ring formation process to be thermodynamically allowed the free energy change ΔG must be negative. Continuum mechanics has been shown by the studies of Yacobson et al.²⁹ to provide a good description of the energetics of structural deformations of carbon nanotubes. The simplest model of the ring formation process consists of a SWNT coiling over itself to form a loop (see inset in Figure 3). By this coiling the tube gains van der Waals adhesion energy, E_B . Opposing this is the strain energy E_S that builds up as a result of the induced curvature. E_S in continuum mechanics is given by³⁰ $E_S = (YI) \cdot l / 2R^2$, where Y is the Young modulus, l is the NT length, R is the loop radius, and $I = (\pi/4)[r^4 - (r - t)^4]$ is the geometrical moment of inertia of a tube having an external radius, r , and a wall thickness t . Thus, the strain energy increases rapidly with decreasing coil radius R . The cohesive energy, E_B , on the other hand, is proportional to the interacting tube length $l_i = l - 2\pi R$. l_i is the excess length of the tube left over after a full single coil has been formed (see inset of Figure 3). This tube segment now interacts with the ring which leads to an adhesion energy $E_B = -Kl_i$ where K is the cohesive energy per length.¹⁸ In addition to the energy changes there are also both positive and negative entropy changes upon ring formation in aqueous environment. Most of that entropy change is due to the presence of "repulsive" hydrophobic interactions between the carbon nanotube and the water solvent (aqueous solution of $H_2SO_4 + H_2O_2$), i.e., there are restrictions on the ability of water to hydrogen-bond near the nanotube–water interface.³¹ Coiling of the tube onto itself decreases the tube–water contact area and thus is favored entropically.

We can now try to estimate the energetic requirements of ring formation and more specifically look at the factors that determine the ring radius distribution. We can formulate this problem as follows: given a tube of length $l = 2\pi R + l_i$, how should this length l be partitioned into R and l_i so that $|E_B| > E_S$. The cohesive energy, K , can be obtained using the values calculated for a nanotube crystal,¹⁸ and $Y = 1$ TPa.³² Figure 3 shows the allowed values of R that would give rise to a thermodynamically stable ring for SWNTs of different tube diameters. It is clear that the critical radius R_C for ring formation is small, especially for thin tubes such as the (10,10) tube ($r = 0.7$ nm). In general, we observe that much lower values of R are allowed by energetics than are observed in the histogram of Figure 1b. Taking the hydrophobic effect into account further reduces R_C . If, instead of using a single SWNT to model the coiling process, we were to use a rope of SWNTs, the thermodynamic stability of the resulting ring would depend on the detailed arrangement of individual NTs in the rope. For a closely packed rope, we calculate an R_C smaller than that for a single SWNT ring.

We may therefore conclude that the process leading to the ring radius distribution observed is not a thermodynamically controlled process. The activation energy ΔE_A (more rigorously the activation free energy) controls the size distribution of the rings. To form a ring the two ends of the tube must first come close to each other. This involves a large amount of strain energy and some initial loss in entropy. Strong adhesion will not develop until the two ends are quite close. These considerations suggest that the activation energy would be large, of the order of the strain energy, and would depend on R roughly as $\Delta E_A \propto$

R^{-2} . Therefore, the large-ring radii observed are kinetically preferred. The required activation energy for the formation of the rings is high (many eV), and is provided in our approach by ultrasonic irradiation. This activation may involve thermal or mechanical effects produced by cavitation, i.e., by the formation and collapse of small bubbles generated by the ultrasonic waves.³³ The large activation energies estimated suggest the involvement of mechanical effects. The nanotubes can act as nucleation centers for ultrasound-induced bubble formation and will be positioned at the bubble–liquid interface as a result of their hydrophobicity. In this position, the nanotube can be mechanically bent as the bubble collapses.

Once formed, a "proto-ring" can grow thicker by the attachment of other pieces of single nanotubes and ropes. This rather random attachment of tubes to the growing ring can account for the typically observed variations in the width of a ring around its circumference. The fact that we find no correlation between the diameter of the rings and their thickness further argues against the relaxation of the initial ring diameter toward its equilibrium configuration. The above discussion also allows us to understand why the nanotubes must be neither too short nor too long to be able to form rings. The formation of a ring from a short "nanotube pipe", although it may be thermodynamically allowed according to the results in Figure 3, will be kinetically improbable. Parts of very long tubes, on the other hand, are likely to come in contact in more than one place, giving a tangle rather than a well-defined ring. This is exactly what is observed in the raw (uncut) SWNT material.¹⁶

Finally, we note that MWNTs usually have a larger diameter than SWNTs so they are less likely to form rings because their much higher flexural rigidity $B (= YI)$ leads to prohibitively high activation energies for the coiling process. Nevertheless, rings of 0.2 to 0.5 μm diameters made from 10 to 20 nm thick MWNT have recently been observed in catalytically grown samples.²⁸ Simple estimates of the thermodynamic stability limits of rings made of larger SWNTs or MWNTs (see examples in Figure 3) indicate that the critical radii of the rings scale with the diameter of the tube and the number of walls inside the tube. This analysis suggests that a 20 nm thick MWNT ring cannot be stabilized by van der Waals forces alone when the ring diameter is less than 0.5 μm . Therefore, the wall structure of the observed MWNT rings is likely to involve defects that twist the nanotube and form the ring. These arguments support the interpretation by Ahlskog et al.²⁸ that pair defects induce the coiling of MWNTs.

We now discuss briefly the electrical properties of SWNT rings. We measured the conductance of SWNT rings by positioning them on lithographically fabricated gold electrodes on top of a layer of SiO_2 grown on a heavily doped Si wafer (Figure 4). The two-probe resistance of the nanotube rings at 300 K ranges from 20 to 50 k Ω . Most of the rings studied had wall thicknesses between 10 and 20 nm, and therefore consist of a bundle of hundreds of nanotubes. This bundle in turn consists of both semiconducting and metallic nanotubes.^{13,14} Because of the poor inter-tube conduction, only the tubes in direct contact with both electrodes contribute to conduction. Figure 4a shows the temperature dependence of the resistance R of a 0.82 μm diameter and 20 nm thick ring. R increases with decreasing temperature T . At first glance, such temperature behavior suggests that the electrical transport at low temperatures is dominated by the semiconducting nanotubes. However, we can rule out this possibility for two reasons. First, there is no

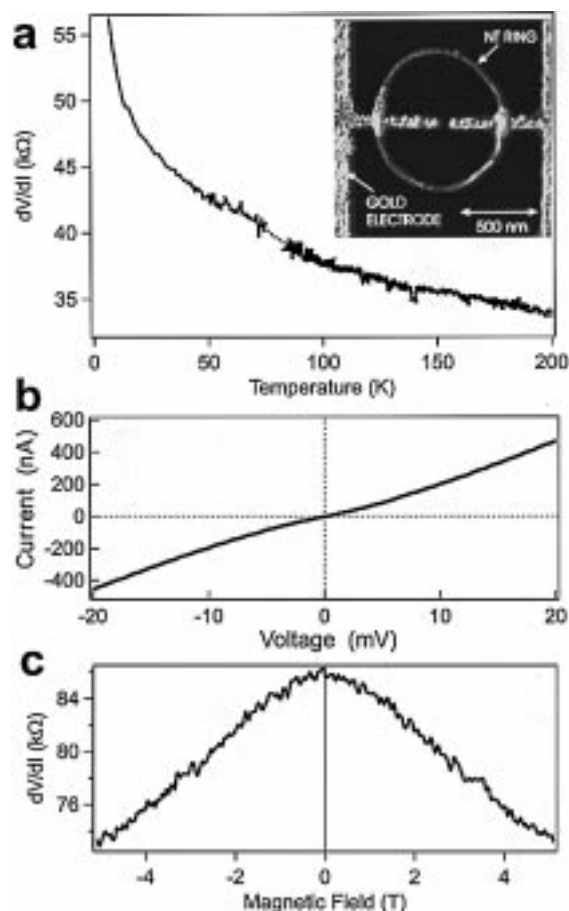


Figure 4. (a) Typical evolution of the resistance as a function of temperature for a SWNT ring. The insert shows an atomic force microscope (AFM) image of a SWNT ring positioned on gold electrodes. (b) Current as a function of bias across the ring at 4 K. (c) Differential resistance, dV/dI , of the nanotube ring as a function of the magnetic field applied perpendicular to the plane of the ring. The probe current was 10 pA. These measurements were performed on a 0.82 μm diameter SWNT ring whose two-terminal resistance at room temperature is 33 k Ω .

effect of the back gate bias on the ring conductance, while a strong conductance modulation is expected for semiconducting nanotubes due to band bending induced by the back gate potential.^{34,35} Second, I – V curves taken at low temperatures (Figure 4b) are essentially linear and do not show a band-gap (the origin of the anomaly near zero bias is discussed elsewhere³⁶).

In general, at low temperatures, we find that electrical transport in the rings is dominated by conduction through metallic nanotubes. The variation of the resistance with temperature presented in Figure 4a is characteristic of a one-dimensional (1D) metallic conductor in a state of weak localization.³⁷ This interpretation is supported by examining the behavior of the resistance in the presence of an external magnetic field perpendicular to the plane of the ring as shown in Figure 4c. The resistance of the ring, in this case at 6 K, decreases with increasing magnetic field over the entire available field range of 0–5 T. This behavior indicates that the ring resistance at low temperatures is dominated by quantum interference phenomena made possible by the ring geometry. An electron wave entering the ring can travel in a clockwise or anticlockwise direction and the two waves interfere back at the injection point. Because tube–tube tunneling is extremely weak, such closed electronic paths must involve electrical coupling between two

overlapping segments of the same tube via a metal electrode, i.e., closed (ring-like) paths involve tube–metal–tube coupling.

As a result of time reversal invariance, the phase shifts acquired along the two Feynman paths are the same, so the two counter-propagating waves interfere constructively at the injection point. In effect, a standing wave is formed which does not contribute to transport. The electron path is effectively increased and so is the number of elastic collisions of the electrons leading to an increased resistance.^{37,38} The quantum interference is destroyed when a magnetic field is applied perpendicular to the ring. The magnetic field lifts the time-reversal invariance so that electrons (or holes) following the two counter-propagating Feynman paths acquire additional opposite phase-shifts, leading to destructive interference, and to the elimination of the quantum mechanical contribution to the resistance. An analysis of magneto-resistance data (such as those shown in Figure 4c) at different temperatures allows the evaluation of the temperature dependence of the coherence length of the electrons and the identification of the dephasing mechanism as will be discussed elsewhere.³⁶

In conclusion, we have developed a procedure by which ring-shaped superstructures of SWNTs can be produced. The formation of these rings is made possible by ultrasonic irradiation of linear nanotube segments, and the resulting rings are stabilized by van der Waals interactions. The combination of materials with unique properties such as the nanotubes with new self-organization schemes opens up the possibility for a host of novel applications. It is known that nanotubes can be functionalized with desired chemical groups and the electronic properties can be changed by doping.³⁹ These capabilities coupled with the self-organization technique presented here provide essential building blocks for new mechanical or electronic devices. NT rings or catenane structures (see Figure 1e) can be used as frames or templates on which new nanostructures can be assembled. Magneto-resistance studies of nanotube rings allow the study of transport mechanisms and electrical properties of nanotubes that are otherwise difficult to access in straight nanotubes.

Acknowledgment. We thank R. E. Smalley and A. G. Rinzler for providing us single-walled nanotubes, L. Gignac for the TEM images, and J. Tersoff for helpful discussions.

References and Notes

- (1) Lehn, J.-M. *Supramolecular chemistry: Concepts and perspectives*; VCH Press: Weinheim, 1995.
- (2) Whitesides, G. M.; Mathias, J. P.; Seto, C. T. *Science* **1991**, 254, 1312.
- (3) Balzani, V.; Gomez-Lopez, M.; Stoddart, J. F. *Acc. Chem. Res.* **1998**, 31, 405.
- (4) Bryson, J. W., et al. *Science* **1995**, 270, 935.
- (5) Creighton, T. E. *Protein folding*; Freeman: New York, 1992.
- (6) Treacy, M. M. J.; Ebbesen, T. W.; Gibson, J. M. *Nature (London)* **1996**, 381, 678.
- (7) Wong, E. W.; Sheehan, P. E.; Lieber, C. M. *Science* **1997**, 277, 1971.
- (8) SWNT rings are comprised of many individual tubes of different sizes and chiralities. As a result, the weak covalent contribution to interlayer adhesion present in graphite should be reduced or eliminated by the incommensurate packing of the tubes forming the ring.
- (9) Iijima, S. *Nature (London)* **1991**, 354, 56.
- (10) Yakobson, B. I.; Smalley, R. E. *Am. Scientist* **1997**, 85, 324.
- (11) Dresselhaus, M. S.; Dresselhaus, G.; Eklund, P. C. *Science of fullerenes and carbon nanotubes*; Academic Press: San Diego, 1996.
- (12) Saito, R.; Fujita, M.; Dresselhaus, G.; Dresselhaus, M. S. *Appl. Phys. Lett.* **1992**, 60, 2204.
- (13) Wildöer, J. W. G.; Venema, L. C.; Rinzler, A. G.; Smalley, R. E.; Dekker, C. *Nature (London)* **1998**, 391, 59.
- (14) Odom, T. W.; Huang, J.-L.; Kim, P.; Lieber, C. M. *Nature (London)* **1998**, 391, 62.

- (15) Bethune, D. S.; Kiang, C. H.; de Vries, M. S.; Goreman, G.; Savoy, R.; Vazquez, J.; Beyer, R. *Nature (London)* **1993**, 363, 605.
- (16) Thess, A., et al. *Science* **1996**, 273, 483.
- (17) Journet, C.; Bernier, P. *Appl. Phys. A* **1998**, 67, 1.
- (18) Tersoff, J.; Ruoff, R. S. *Phys. Rev. Lett.* **1994**, 73, 676.
- (19) Hertel, T.; Martel, R.; Avouris, Ph. *J. Phys. Chem. B* **1998**, 102, 910.
- (20) Hertel, T.; Walkup, R. E.; Avouris, Ph. *Phys. Rev. B* **1998**, 58, 13870.
- (21) Falvo, M. R., et al. *Nature (London)* **1997**, 389, 582.
- (22) Liu, J., et al. *Science* **1998**, 280, 1253.
- (23) Martel, R.; Shea, H. R.; Avouris, Ph. *Nature (London)* **1999**, 398, 299.
- (24) Wasserman, S. A.; Cozzarelli, N. R. *Science* **1986**, 232, 951.
- (25) Wong, S. S.; Joselevich, E.; Woolley, A. T.; Cheung, C. L.; Lieber, C. M. *Nature (London)* **1998**, 394, 52.
- (26) Liu, J., et al. *Nature (London)* **1997**, 385, 780.
- (27) McEuen, P. Personal communication reported by Vossmeier, T., et al. *Adv. Mater.* **1998**, 10, 351.
- (28) Ahlskog M., et al. *Chem. Phys. Lett.* **1999**, 300, 202.
- (29) Yakobson, B. I.; Brabec, C. J.; Bernholc, J. *Phys. Rev. Lett.* **1996**, 76, 2511.
- (30) See, for example, Barber, D. J.; Loudon, R. *An introduction to the properties of condensed matter*; Cambridge University Press: Cambridge, 1989.
- (31) Tanford, C. *The hydrophobic effect*; J. Wiley: New York, 1980.
- (32) Lu, J. P. *Phys. Rev. Lett.* **1997**, 79, 1297.
- (33) *Ultrasound: Its chemical, physical and biological effects*; Suslick, K. S., Ed.; VCH Publishers: Weinheim, 1988.
- (34) Tans, S.; Vershueren, A. R. M.; Dekker, C. *Nature (London)* **1998**, 393, 49.
- (35) Martel, R.; Schmidt, T.; Shea, H. R.; Hertel, T.; Avouris, Ph. *Appl. Phys. Lett.* **1998**, 73, 2447.
- (36) Shea, H. R.; Martel, R.; Avouris, Ph. Submitted.
- (37) For reviews, see Bergmann, G. *Phys. Rep.* **1984**, 107, 1; Lee, P. A.; Ramakrishnan, T. V. *Rev. Mod. Phys.* **1985**, 57, 287.
- (38) Aronov, A. G.; Sharvin, Yu. V. *Rev. Mod. Phys.* **1987**, 59, 755.
- (39) Carroll, D. L.; Redlich, Ph.; Blasé, X.; Charlier, J.-C.; Curran, S.; Ajayan, P. M.; Roth, S.; Rühle, M. *Phys. Rev. Lett.* **1998**, 81, 2332.